ACCOUNTS of chemical research

Article

Cite This: Acc. Chem. Res. 2018, 51, 1054−1062

pubs.acs.org/accounts

Principles and Methods for the Rational Design of Core−Shell Nanoparticle Catalysts with Ultralow Noble Metal Loadings

Sean T. Hunt* and Yuriy Román-Leshkov*

Department of Chemical Engineering, Massachusetts Institute of Technology, Cambridge, Massachusetts 02139, United States

CONSPECTUS: Commercial and emerging renewable energy technologies are underpinned by precious metal catalysts, which enable the transformation of reactants into useful products. However, the noble metals (NMs) comprise the least abundant elements in the lithosphere, making them prohibitively scarce and expensive for future global-scale technologies. As such, intense research efforts have been devoted to eliminating or substantially reducing the loadings of NMs in various catalytic applications. These efforts have resulted in a plethora of heterogeneous NM catalyst morphologies beyond the traditional supported spherical nanoparticle. In many of these new architectures, such as shaped, high index, and bimetallic particles, less than 20% of the loaded NMs are available to perform catalytic turnovers. The majority of NM atoms are subsurface, providing only a secondary catalytic role through geometric and ligand effects with the active surface NM atoms. A handful of architectures can approach 100% NM utilization, but severe drawbacks limit general applicability. For example, in addition to problems with stability and leaching, single atom and ultrasmall cluster catalysts have extreme metal−support interactions, discretized d-bands, and a lack of adjacent NM surface sites. While monolayer thin films do not possess these features, they exhibit such low surface areas that they are not commercially relevant, serving predominantly as model catalysts.

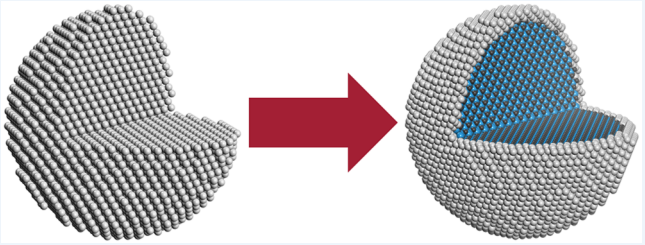

This Account champions core−shell nanoparticles (CS NPs) as a vehicle to design highly active, stable, and low-cost materials with high NM utilization for both thermo- and electrocatalysis. The unique benefits of the many emerging NM architectures could be preserved while their fundamental limitations could be overcome through reformulation via a core−shell morphology. However, the commercial realization of CS NPs remains challenging, requiring concerted advances in theory and manufacturing. We begin by formulating seven constraints governing proper core material design, which naturally point to early transition metal ceramics as suitable core candidates. Two constraints prove extremely challenging. The first relates to the core modifying the shell work function and d-band. To properly investigate materials that could satisfy this constraint, we discuss our development of a new heat, quench, and exfoliation (HQE) density functional theory (DFT) technique to model heterometallic interfaces. This technique is used to predict how transition metal carbides can favorably tune the catalytic properties of various NM monolayer shell configurations. The second challenging constraint relates to the scalable manufacturing of CS NP architectures with independent synthetic control of the thickness and composition of the shell and the size and composition of the core. We discuss our development of a synthetic method that enables high temperature self-assembly of tunable CS NP configurations. Finally, we discuss how these principles and methods were used to design catalysts for a variety of applications. These include the design of a thermally stable sub-monolayer CS catalyst, a highly active methanol electrooxidation catalyst, CO-tolerant Pt catalysts, and a hydrogen evolution catalyst that is less expensive than state-of-the-art NM-free catalysts. Such core−shell architectures offer the promise of ultralow precious metal loadings while ceramic cores hold the promise of thermodynamic stability and access to unique catalytic activity/tunability.

INTRODUCTION

Spanning energy, fine chemicals, plastics, agriculture, and environmental control, heterogeneous catalytic processes drive over 30% of global GDP and account for over 90% of all chemical processes.[1−3] The heterogeneous catalyst market was $20 billion in 2015, and these materials enabled more than $20 trillion in global sales.[4,5] By contributing less than 0.1% to the costs of their products, heterogeneous catalysts accelerate not only chemical reactions, but our modern economy.

Catalysts containing noble metals (NMs) account for more than 70% of the global heterogeneous catalyst market.[5] These scarce and expensive resources are ubiquitous in industrial catalysis due to their unparalleled catalytic activity and durability. For many processes, there are simply no alternatives. Historically, the heterogeneous catalysis market grows by 8% per year.[5] However, NM catalyst demand is set to far outpace this historical growth rate (by up to 45% per year)[6] due to renewable energy and green chemistry applications on the horizon. The scarcity and cost of NMs has led many to question the economic feasibility of an ever-expanding role for precious metal catalysts.[6−9]

One solution is to develop new NM catalyst architectures that maximize activity and durability while minimizing precious

Received: October 13, 2017
Published: March 6, 2018

DOI: 10.1021/acs.accounts.7b00510
Acc. Chem. Res. 2018, 51, 1054−1062

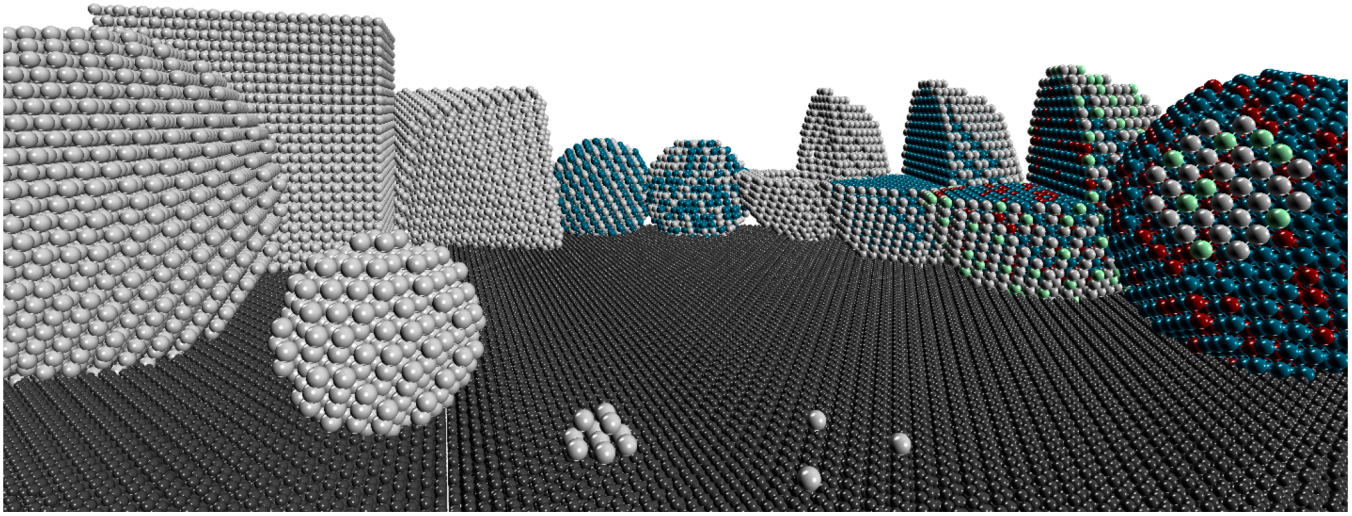

Figure 1. Emerging noble metal catalyst architectures supported on graphitic carbon (drawn to scale). Shown clockwise from front center are single Pt atoms, a 10 atom Pt cluster, a 2 nm Pt NP, a 5 nm Pt NP, a 6 nm Pt cube, a 6 nm Pt octahedron, a 4 nm intermetallic NP, a 4 nm random alloy NP, a 5 nm hollow Pt NP, a 5 nm CS NP, a 5 nm heterometallic CS NP, and a 5 nm sub-monolayer heterometallic CS NP.

metal usage. This requires concerted advances in theory, synthesis, and scalable catalyst manufacturing. Within the landscape of emerging catalyst architectures, this Account offers monolayer core−shell nanoparticles (CS NPs) as a general and tunable design platform for both emerging renewable energy applications as well as established industrial processes.

However, there are many synthetic challenges and constraints on the core material formulation. As such, designing active, stable, and inexpensive CS NPs has remained elusive. From computational simulations and model thin film catalysts, to achieving a tunable CS NP synthetic platform, this Account describes the design of transition metal ceramic (TMC) NPs as ideal core substrates for supporting NM monolayer shells. Although many challenges remain, this development offers a new path toward the design of low-cost, next generation NM catalysts for applications across both thermo- and electro-catalysis.

EMERGING NOBLE METAL CATALYST DESIGN STRATEGIES

The ultimate goal in catalytic design is to have complete synthetic control of the material properties that determine reactivity, selectivity, and stability.[7,10,11] Although the traditional NM catalyst engineering tool kit is ill-equipped to optimize these parameters, advances in synthetic techniques are rapidly making new catalyst designs accessible. Figure 1 depicts a variety of emerging NM nanostructures (drawn to scale) adsorbed on a graphitic carbon support.

Currently, commercial heterogeneous NM catalysts are formulated almost exclusively as small NPs (less than 10 nm) dispersed on a high surface area oxide (e.g., silica or alumina) or a carbonaceous support. The 2 and 5 nm Pt NPs in Figure 1 are typical of what might be found in a standard Pt/C commercial catalyst, with 2 nm particles offering better dispersion and 5 nm particles offering better stability.[12] Although these catalysts are simple to synthesize, they offer few "levers" for tuning catalytic reactivity. They remain susceptible to several deactivation mechanisms, including poisoning, coking, sintering, dissolution, leaching, and support degradation.[13−15]

To address the problems of traditional heterogeneous NM catalysts, many exciting new architectural directions are now under investigation (Figure 1). Although susceptible to sintering and leaching, single-atom catalysts and clusters offer exceptional dispersion and unique reactivity due to d-band discretization and the absence of multiple adjacent metal sites. While these structures exhibit high NM dispersion, the absence of adjacent NM sites and high coordinative unsaturation may not be suitable for many reactions. Conversely, shaped catalysts are dominated by singular facets and poor dispersion. Long-term durability of both architectures tends toward traditional spherical particles, which exhibit the minimum in surface free energies.[16] The predisposition of most architectures to tend toward spherical particles also hampers the use of hollow nanoparticles, especially at elevated temperatures.[17]

Bimetallic NPs are a mainstay in NM catalyst engineering.[18] They can be synthesized in three forms depending on the elements used and the synthesis conditions: Janus-type (not shown), random alloys, and ordered intermetallic alloys (Figure 1). These architectures feature high metal dispersion and near limitless design pathways for achieving bifunctional surfaces and/or more stable catalysts. By alloying NMs with earth-abundant materials, the overall catalyst cost can also be reduced.

Of the structures depicted in Figure 1, CS NPs offer the most design flexibility.[10] For instance, CS NPs can be tuned by size, shape, heterometallic core composition, and heterometallic shell composition. Even the shell thickness can be tuned from single atoms to a full monolayer (ML) or to several multilayers of coverage. This tunability enables complete control over the NM dispersion, regardless of particle size. Although it is easy to envision the CS NPs in Figure 1, this level of precise synthetic control remains elusive, especially at tonne scales.[19,20]

CONSTRAINTS ON THE CORE MATERIAL

In our pursuit of rationally designed catalysts, we began investigating this architecture by first limiting the design space to an ideal CS NP, one that could be optimized for many reactions in both thermo- and electro-catalysis. With this objective, selection of the ideal core material becomes rigorously constrained (Table 1).[21] Currently, there are no known core materials that satisfy all of the constraints in Table

DOI: 10.1021/acs.accounts.7b00510
Acc. Chem. Res. 2018, 51, 1054−1062

Table 1. Constraints on the Ideal Core Material

1.	earth-abundant and inexpensive
2.	metallic electrical conductivity and acidic/alkaline corrosion resistance
3.	melting point > 2000 °C
4.	shell material is insoluble in the core lattice
5.	shell monolayer formation on the core is favorable, and interfacial bonding is strong
6.	core has minimal or favorable modifications to shell work function and d-band
7.	readily manufactured and independently tunable core−shell architectures

1, but satisfying these constraints is critical to achieving a general and commercially relevant CS architecture.

Constraints 1−3

First, the core must be earth-abundant and inexpensive to minimize cost by maximizing NM dispersion in the shell. For use as an electrocatalyst, the core must be electrically conductive to minimize ohmic losses. The core must also be corrosion-resistant in both acidic and alkaline media to mitigate leaching/dissolution of the core over time.

Whereas coked catalysts can be regenerated via high temperature heat treatments (e.g., calcination), sintered catalysts instead require complete recovery and resynthesis ex situ. Sintering occurs rapidly above the Tammann temperature of a material, which is roughly one-third of the melting point. Because many commercial reactions operate at or above 600 °C, an ideal core substrate requires a melting point above 2000 °C to achieve a sinter-resistant CS NP catalyst.

Constraint 4

Currently, late 3d transition metals, such as Fe, Co, Ni, and Cu, are common core materials for supporting NM monolayers. However, these materials are not corrosion resistant in both acidic and alkaline media. Furthermore, their melting points are well below 2000 °C. With respect to constraint 4 in Table 1, NMs are soluble in late 3d transition metal lattices. This precludes these core materials from use in thermal catalysis or high temperature regeneration procedures. Even at lower temperatures, substantial mixing of the shell and core material can occur over the catalyst lifetime due to nonzero interlattice diffusivities.[17] As shown in Figure 2, a CS NP occupies a specific configuration and is therefore in a low entropy state. As such, a thermodynamically stable CS architecture is only achievable if the shell is insoluble in the core lattice.

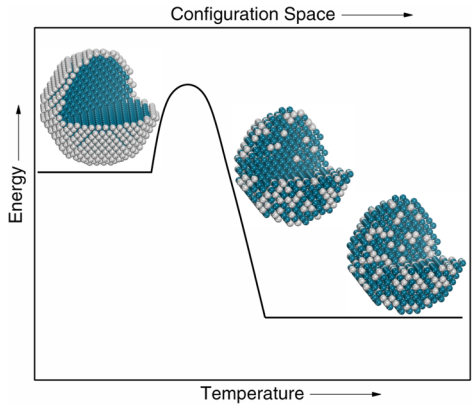

Figure 2. Core−shell structures are metastable if the shell is soluble in the core lattice. Adapted with permission from ref 21. Copyright 2016 Massachusetts Institute of Technology Press.

Constraints 5−7

To satisfy both Constraints 4 and 5 in Table 1, the NM shell must be both insoluble in the core lattice ($\Delta G_{mix} > 0$) but also exhibit a strong interfacial bonding interaction between the shell and the core ($\Delta G_{C-S} < \Delta G_{S-S}$). If this interfacial interaction is weak, the shell could leach from the surface or phase-separate to form a Janus-type particle.

Strong interfacial bonding also implies charge transfer of electron density between the shell and the core. To maintain catalytic activity of the shell, especially at only a single monolayer of coverage or lower, the shell work function (metallic Fermi level) and the shell d-band must be minimally altered by the core material. Ideally, the core should offer tunable pathways for favorably modulating the d-band structure and work function of the NM shell to improve activity/selectivity.

The final constraint in Table 1 is practical rather than fundamental. To have complete control over the material properties that govern reactivity, engineers need the ability to control the shell thickness and its heterometallic composition independently from the core diameter and its heterometallic composition. This must be achievable using scalable synthetic methods to minimize manufacturing costs. This final constraint is critical for CS NPs to be both rationally designed and commercially relevant catalysts.

TRANSITION METAL CERAMICS AS IDEAL CORE CANDIDATES

Early TMCs comprise elements from Groups 4, 5, and 6 of the periodic table with a nonmetal (e.g., C, N, P, etc.) intercalated into the interstitial sites of the parent metal. These ceramic materials exhibit many promising topochemical properties to satisfy the core constraints outlined in Table 1. First, they are earth-abundant and exhibit fully metallic electrical conductivities with melting points exceeding even 3000 °C in some instances.[22] Second, it has been shown that many TMCs exhibit corrosion-resistance over wide potential windows in both acidic and alkaline media, in particular WC, TiC, TaC, and ZrC.[23] Due to their unique properties, there is already widespread commercial use of TMCs in a variety of applications.[22]

The catalytic surface chemistries of TMCs have been under investigation for decades, beginning with the landmark study by Levy and Boudart, which suggested that pristine WC exhibits "Pt-like" catalytic reactivity.[24] More recently, it has been shown that TMCs are distinct catalysts that enable unique reaction pathways, especially when the surface is passivated with an oxide layer.[25,26] Currently, the unique reaction pathways on pristine TMC surfaces is best explained by density functional theory (DFT) comparisons of oxygen and carbon binding energies on TMC surfaces, which show a marked departure from the traditional "scaling relations" of transition metals.[27]

Due to their unique and sometimes "NM-like" surface chemistries, TMCs have already been investigated as supports and/or cocatalysts for NM NPs in numerous studies where they have been found to improve or modulate the activity and stability of traditional NM NP catalysts.[28−30] These studies suggest useful synergies between NMs and TMCs, but they also hint at a more fundamental property of TMCs. Regardless of how the catalysts were formulated in these studies, the NMs were never observed to alloy with the TMCs, suggesting that

DOI: 10.1021/acs.accounts.7b00510
Acc. Chem. Res. 2018, 51, 1054−1062

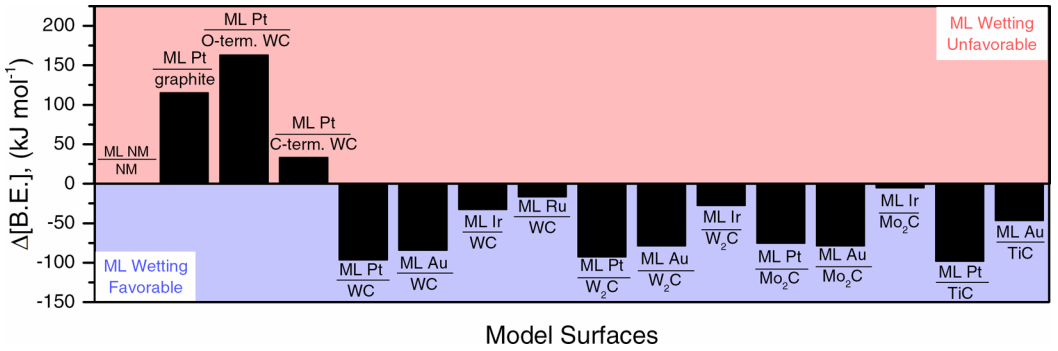

Figure 3. Interfacial binding energy difference of various noble metal monolayers on various substrate surfaces. Adapted with permission from ref 35. Copyright 2016 American Association for the Advancement of Science.

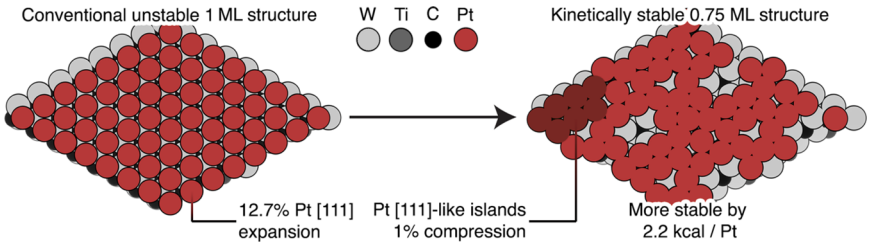

Figure 4. HQE method shows that the conventional 1 ML Pt/TiWC interfacial model is a local thermodynamic energy minimum. Its global thermodynamic energy minimum is a compressed 0.75 ML Pt/TiWC structure comprised of Pt[111]-like islands. Adapted with permission from ref 36. Copyright 2016 American Chemical Society.

they are insoluble. Computational studies and direct experimental evidence also reveal that NMs will not readily form carbides or nitrides.[31] This suggests that TMCs satisfy Constraint 4 in Table 1.

Unfortunately, these studies also imply that the remaining constraints in Table 1 are not satisfied by TMCs. Neither monolayer wetting of NMs on nanostructured TMC surfaces nor CS NPs were achieved in these reports. Although this could suggest that NM-TMC interfacial bonding is weak/unfavorable, these studies do not agree with thin film studies on model surfaces, which showed that NM monolayers will wet *metal-terminated* TMC surfaces and maintain catalytic activity.[32−34]

To investigate this discrepancy, we used simple DFT calculations to examine the interfacial bonding energetics of NM monolayers on model TMC surface slabs (Figure 3).[35] Here, Δ[BE] is the difference in binding energy between a NM monolayer on its native NM (111) surface and a probe surface slab (denoted as *X*):

$$\Delta[\mathrm{BE}] = \Delta[\mathrm{BE}_{\mathrm{MLNM/NM}} - \mathrm{BE}_{\mathrm{MLNM}/X}]$$

Figure 3 shows that monolayer formation is favorable for a variety of NM monolayers on different TMC slabs. However, NM/TMC (shell/core) wetting is favorable only when the TMC surface is *metal-terminated*. In the case of Pt/WC where the WC surface is terminated with carbidic C or an oxide passivation layer, monolayer formation is not predicted to be favorable, just as Pt/graphite monolayer formation is also not favorable (Figure 3).

Although DFT suggests monolayer NM/TMC interfacial bonding is favorable on metal-terminated surfaces, CS NPs had never been synthesized. Furthermore, it was unknown how a TMC core would affect the d-band and work function of a NM shell. With respect to the final three constraints in Table 1, we sought to develop new computational and synthetic methods to determine if TMC NPs could serve as ideal substrates for NM monolayers.

HQE: A NEW TECHNIQUE TO MODEL HETEROMETALLIC INTERFACES

Finding Global Minima

To predict catalytic activity and guide rational synthetic design, we needed accurate descriptions of heterometallic NM/TMC interfaces. Traditionally, such interfaces are modeled by depositing a stoichiometric NM adlayer on top of either the octahedral or tetrahedral TMC surface sites, as shown in Figure 4. This results in a 1:1 ratio of surface NM atoms to subsurface metal atoms, with the NM atoms occupying points of high crystallographic symmetry. However, these calculations are done at 0 K in a perfect vacuum. There is no a priori justification that a monolayer NM/TMC surface need be so symmetric. This is especially suspect when considering that this high symmetry configuration results in a 12.7% lattice expansion of Pt (Figure 4).

In reality, monolayer NM/TMC catalysts are both synthesized and operated at elevated temperatures where the NM will equilibrate with the subsurface TMC. To model NM/TMC interfaces accurately, we developed the Heat, Quench, and Exfoliate (HQE) method by coupling DFT with molecular dynamics (MD).[36] This method reveals that the conventional 1 ML Pt/TiWC surface from Figure 4 is not the thermodynamic minimum energy structure. Instead, this surface transforms into a more stable (by 2.2 kcal/Pt) 0.75 ML structure consisting of small Pt islands with 1% compression rather than the 12.7% lattice expansion predicted by the conventional slab. HQE can reveal global thermodynamic minima rather than local minima.

Predicting Work Function and d-Band Modifications

This new method allowed proper investigation of constraint 6 in Table 1 for a variety of NM configurations on TiWC.[36] For

DOI: 10.1021/acs.accounts.7b00510
Acc. Chem. Res. 2018, 51, 1054−1062

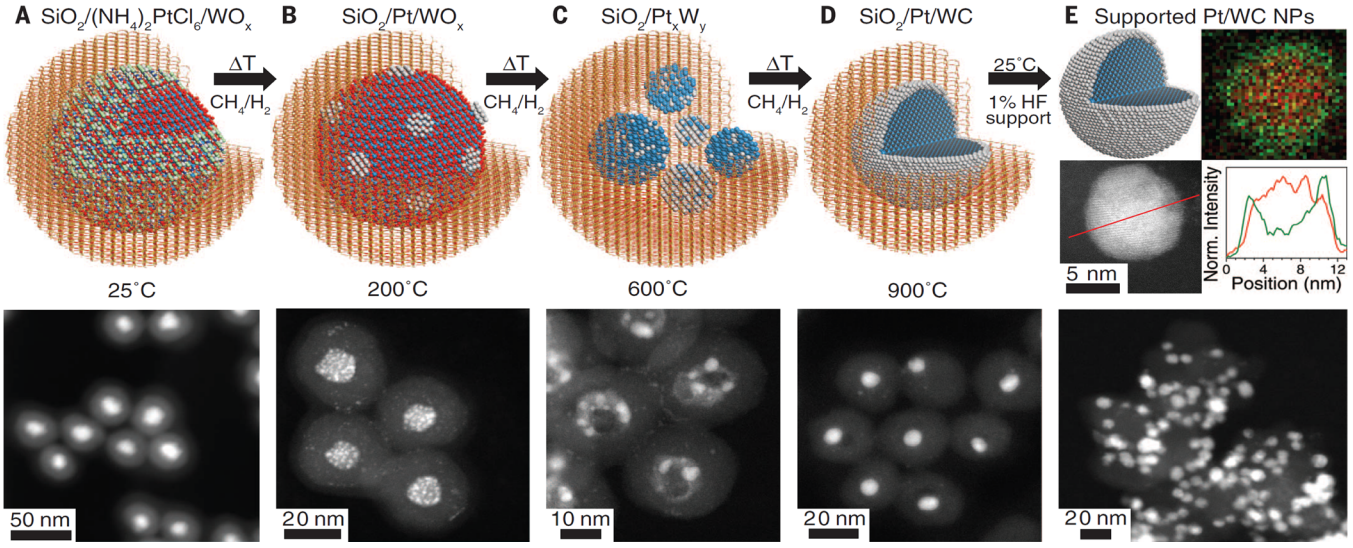

Figure 5. Temperature-dependent self-assembly of Pt/WC (shell/core) nanoparticles. Adapted with permission from ref 35. Copyright 2016 American Association for the Advancement of Science.

most NMs, a TiWC substrate is not predicted to appreciably alter the NM work function. Because kinetic rates in metal-catalyzed reactions can exhibit exponential dependence on the metal work function,[37] it is critical to design a core material that minimally alters the intrinsic NM work function.

Catalytic activity has also been strongly correlated to the first moment of the d-band density of states (i.e., the d-band center).[38] Negative d-band center shifts correlate with weakened adsorption enthalpies of common poisons, such as CO, and are considered favorable for many reactions. Conversely, positive d-band center shifts are correlated with stronger reagent binding, which could be desirable in certain applications. The HQE method revealed that a TiWC substrate could be used to finely tune the d-band center of a monolayer shell. For NM configurations of Pd, Pt, Au, and Sn, a TiWC substrate is predicted to considerably downshift the metal d-band center, potentially improving activity, selectivity, and resistance to common catalyst poisons for many reactions.[36] Ultimately, our goal was to test this prediction experimentally once we had developed a synthetic method capable of realizing NM/TMC NPs.

■ ENABLING NM/TMC SELF-ASSEMBLY

Achieving Nonsintered, Metal-Terminated TMC NPs

Taken together, the HQE/DFT studies and prior model thin film studies suggest that TMCs could serve as ideal cores for supporting NM monolayer CS NPs. Given that NM/TMC NPs could only form in the presence of metal-terminated TMC surfaces (Figure 3), our first goal was to develop a new synthetic method capable of achieving size-tunable, metal-terminated TMC NPs.[39,40] To prevent sintering while mitigating excess carbon deposition, metal oxide precursor NPs were encased in removable silica nanospheres using a reverse microemulsion. During carburization in a CH_4/H_2 atmosphere, the silica remained porous to the carburizing/reducing gases while also mitigating TMC sintering.[41] After carburization, the silica shells were removed in fluoride-containing media, and the nonsintered, metal-terminated TMC NPs were adsorbed onto a traditional catalyst support, such as carbon black.

By tuning the silica to metal oxide precursor ratios and the carburization conditions, we also showed that this method can control the crystalline phase and the average particle size distribution (PSD). Co-hydrolysis of different metal oxide precursors allowed us to synthesize bimetallic TMC NPs. We found that $Ta_{0.3}W_{0.7}C$ exhibited improved electrochemical oxidation resistance without sacrificing HER activity.[42] X-ray absorption fine structure (XAFS) studies demonstrated that the $Ta_{0.3}W_{0.7}C$ NPs were well-mixed random alloys in a compressed lattice similar to the random alloy bimetallic NP shown in Figure 1.[42] These results also informed how TMCs were modeled using our HQE method.

Unsuccessful NM/TMC Attempts

Although this new method enabled the first tunable syntheses of metal-terminated monometallic and heterometallic carbide NPs, controlled deposition of NM monolayers remained nontrivial. Unless exposure to air and water is rigorously prevented, the TMC NPs will passivate. Several attempts were made to deposit Pt monolayers onto metal-terminated WC NPs using methods such as atomic layer deposition (ALD) and reduction of hexachloroplatinic acid onto a nonaqueous WC colloidal suspension. However, these methods proved cumbersome and ineffective. Pt would often deposit unselectively, and the extra processing steps added undesired synthetic complexity.

The Self-Assembly Hypothesis

Instead, we posited that constraint 4 in Table 1 could be exploited to enable an elegant self-assembly process. We knew from our prior studies that after carburization in a CH_4/H_2 atmosphere, pristine metal-terminated TMCs are achieved due to hydrogen scavenging.[33] If we could engineer controlled quantities of NMs to be near each TMC NP within the silica nanospheres, then CS NPs should self-assemble after carburization per our computational predictions. Rather than adding a postsynthetic deposition step, we could achieve this goal by simply modifying our existing synthetic framework. Before encapsulating the metal oxide precursors in a silica shell, we found that NM salts could be uniformly deposited onto each metal oxide NP within the reverse microemulsion. However, several questions remained. It was uncertain if the

DOI: 10.1021/acs.accounts.7b00510
Acc. Chem. Res. 2018, 51, 1054−1062

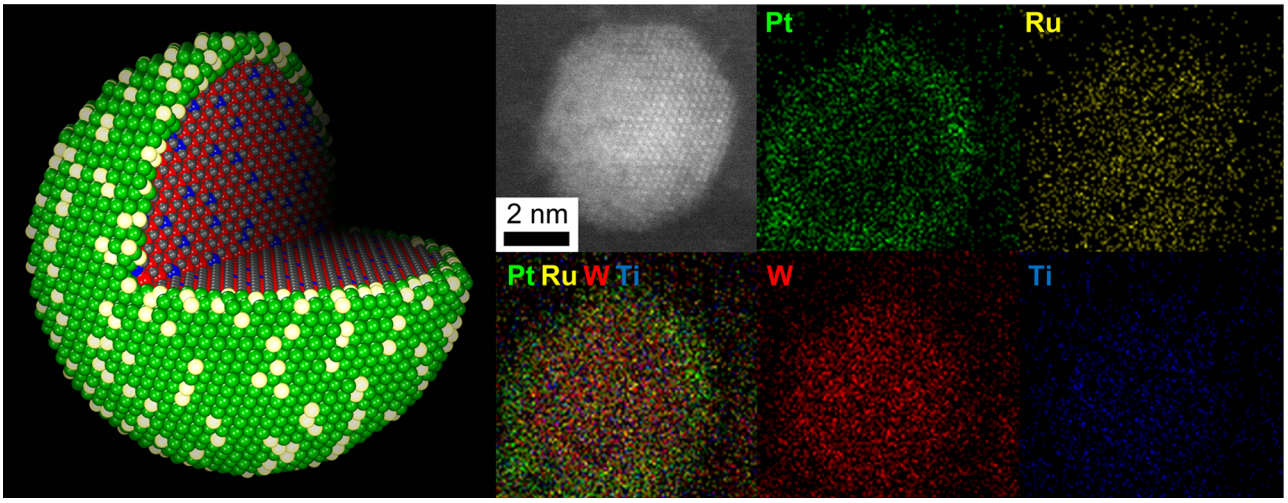

Figure 6. STEM-EDX maps of a 2−3 monolayer $Pt_{0.67}Ru_{0.33}/Ti_{0.1}W_{0.9}C$ (denoted as PtRu/TiWC) nanoparticle and an accompanying cut-away model of the nanoparticle. Adapted with permission from ref 35. Copyright 2016 American Association for the Advancement of Science.

silica nanospheres would be able to mitigate sintering and coke deposition with highly active and low melting point NMs encapsulated. It was also unclear if the metals would dealloy and self-assemble into CS NPs under such extreme carburizing conditions.

The Self-Assembly Process

To probe our hypothesis, we used scanning transmission electron microscopy (STEM) coupled with energy dispersive X-ray spectroscopy (EDX) to observe the Pt/WC self-assembly process at various stages of the carburization heat treatment (Figure 5).[35] After separation from the reverse microemulsion, the as-synthesized wet cake showed distinct ca. 30 nm SiO_2 nanospheres encapsulating an amorphous ca. 10 nm $(NH_4)_2PtCl_6/WO_x$ core (Figure 5A). Because Pt is easier to reduce than WO_x, small Pt^0 islands were observed at 200 °C on the WO_x surface (Figure 5B) in a CH_4/H_2 atmosphere. By 600 °C, WO_x also reduced (Figure 5C), resulting in a polydisperse array of W^0 and Pt^0 NPs encapsulated within the SiO_2 nanospheres. Since WO_x is nearly 3-fold less dense than W^0, the SiO_2 nanospheres become hollow, with the W^0 and Pt^0 NPs adsorbed to the inner walls.

Between 600 and 900 °C, three separate processes drive the final observed transformation (Figure 5D). First, the rates of methane decomposition and solid-state diffusion of C into the W^0 lattice become appreciable, causing carburization of the W^0 moieties into WC. Second, the insolubility of Pt in WC drives phase separation of Pt from the WC lattice. Lastly, the high temperatures cause the discrete NPs to sinter within the hollow SiO_2 nanosphere. Because this method enables Pt to be in close proximity to metal-terminated WC NPs, the phase-separated Pt wets the WC NP, forming Pt/WC (shell/core) NPs. After cooling, the SiO_2 was removed in fluoride media, and the Pt/WC NPs were dispersed on a traditional carbon support (Figure 5E).

Effectively, the silica nanospheres enable the self-assembly of CS NPs by serving as nanoreactors. They allow the bulk metal composition (determined by inductively coupled plasma mass spectrometry [ICP-MS]) to be equivalent to the individual nanoparticle composition. Because the self-assembly process concentrates NMs in the shell and non-NMs in the core, this synthetic framework enables the design of highly complex CS architectures without additional synthetic complexity. An example is shown in Figure 6 where the method was used to create NM/TMC NPs with 2−3 monolayer shells of $Pt_{0.67}Ru_{0.33}$ on $Ti_{0.1}W_{0.9}C$ cores. Recently, we have extended this method to include transition metal nitride cores.[43]

THERMAL STABILITY AND ELECTROCATALYTIC PROPERTIES OF NM/TMC NANOPARTICLES

Thermal Stability

After developing the first method capable of making bespoke NM/TMC nanoparticles, we sought to determine experimentally if this new class of materials satisfied Constraints 4−6 in Table 1. As the synthetic method uses operating temperatures of 900 °C, it is now clear that NMs are poorly soluble in TMC

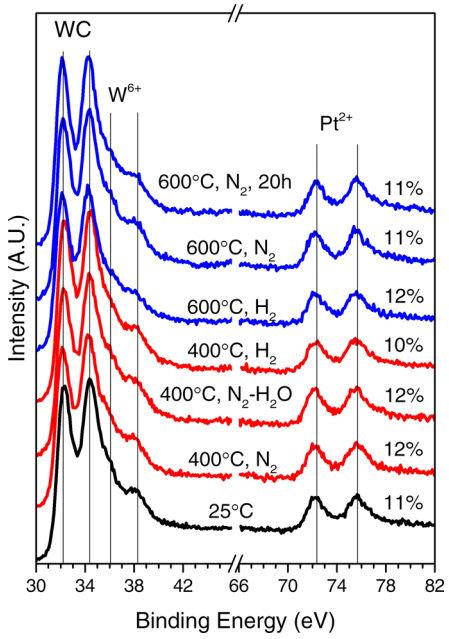

Figure 7. XPS Pt:W ratios of 1/4 ML Pt/TiWC nanoparticles supported on carbon after exposure to various heat treatments in different atmospheres. Adapted with permission from ref 35. Copyright 2016 American Association for the Advancement of Science.

DOI: 10.1021/acs.accounts.7b00510
Acc. Chem. Res. 2018, 51, 1054−1062

lattices, even at high temperatures. To probe Constraints 4 and 5 further, we prepared carbon-supported 3−4 nm $Ti_{0.1}W_{0.9}C$ NPs coated with only 1/4 ML Pt shells and subjected them to heat treatments up to 600 °C in various atmospheres (dry N_2, dry H_2, and H_2O-saturated N_2).[35] In this sub-monolayer configuration, all Pt is at the surface and therefore passivated as PtO, which is detectable as Pt^{2+} via XPS. Furthermore, the XPS-determined Pt:W ratios were enriched (ca. 11%) relative to the ICP-MS-determined Pt:W ratios, confirming the core−shell nature of these particles. After each heat treatment, negligible changes were observed in the Pt oxidation state nor the Pt:W ratios (Figure 7).[35] This suggests that even sub-monolayer Pt/TiWC nanoparticles are thermally stable with strong interfacial bonding.

CO Tolerance

Next, we used our HQE/DFT predictions to guide the experimental design of CS NPs with improved electrocatalytic activity and stability with reduced NM loadings. HQE predicts a substantial downshift of the Pt d-band center in both Pt/TiWC and Pt/TiWN. This should correspond to a ca. 9.6 kcal mol^{-1} weakening of the CO binding energy on Pt surface sites. To probe this prediction, we examined the CO tolerance of Pt/TiWC and Pt/TiWN CS NPs during hydrogen oxidation (HOR). Whereas commercial Pt/C exhibits a ca. 400 mV onset potential for HOR in the presence of 1000 ppm of CO, Pt/TiWC and Pt/TiWN exhibit less than a ca. 50 mV onset potential (Figure 8). The improved CO tolerance of Pt/TiWN in comparison to Pt/TiWC demonstrates the ability to tune the Pt monolayer surface d-band center by altering the core material.[43]

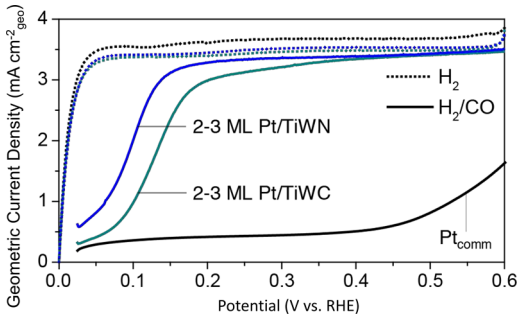

Figure 8. In comparison to commercial Pt/C, Pt/TiWC and Pt/TiWN exhibit increased CO tolerance during HOR in the presence of 1000 ppm of CO. Adapted with permission from ref 43. Copyright 2017 John Wiley and Sons.

Methanol Electrooxidation (MOR)

This intrinsic CO tolerance lends itself to improved MOR activity for both Pt/TiWC and PtRu/TiWC where adsorbed CO is a rate-limiting intermediate. Pt/TiWC exhibited a ca. 60 mV reduction in onset potential compared to commercial Pt/C (Figure 9). Commercial PtRu/C has an extremely low onset potential of ca. 250 mV, governed by the formation of adsorbed OH species on Ru. PtRu/TiWC (Figure 6) shows a similarly low onset potential but with substantially improved kinetics (Figure 9). For instance, the turnover frequency (TOF) of PtRu/TiWC was improved by a factor of 4 at 0.6 V as compared to PtRu/C.[35] After 10 000 electrochemical cycles and alkaline regeneration, the PtRu/TiWC exhibited a factor of 11 improvement in TOF as compared to PtRu/C. Together, these electrocatalytic studies indicate that ceramic cores can improve

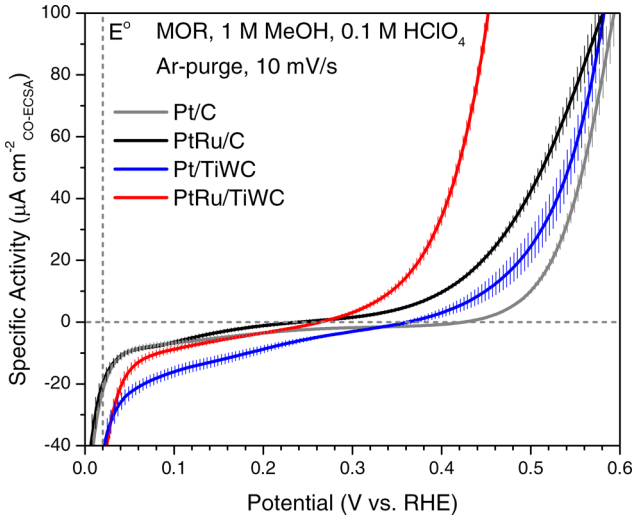

Figure 9. In comparison to their commercial counterparts, Pt/TiWC and PtRu/TiWC exhibit improved MOR activity. Adapted with permission from ref 35. Copyright 2016 American Association for the Advancement of Science.

both the activity and the stability of NM monolayers while reducing NM loadings.

Core−Shell Nanoparticles vs Model Thin Films

Our new method also allowed us to examine the structure-sensitivity differences between a high surface area CS NP architecture and model thin films. Previously, a study of the hydrogen evolution reaction (HER) on polycrystalline Pt/WC thin films showed that only a single monolayer of Pt was required to achieve the HER activity of a Pt foil (Figure 10).[32] Sub-monolayer Pt/WC thin film configurations were orders of magnitude less active than the Pt foil. In contrast, only 1/4 monolayer coverage was required for Pt/TiWC CS NPs to

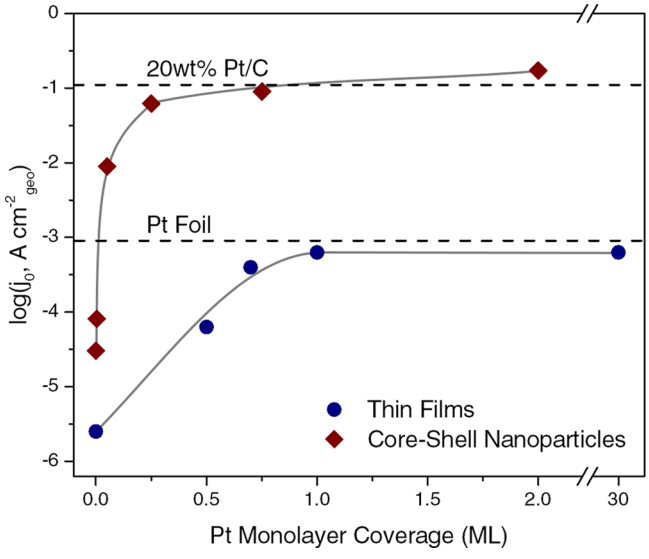

Figure 10. HER exchange current density vs monolayer Pt coverage for thin films of Pt/WC (in 0.5 M H_2SO_4)[32] in comparison to Pt/TiWC CS NPs (in 1.0 M $HClO_4$).[44] The exchange current density of commercial Pt foil and 20 wt % Pt/C is shown for reference. Adapted with permission from ref 32. Copyright 2010 John Wiley and Sons. Adapted with permission from ref 44. Copyright 2016 Royal Society of Chemistry.

DOI: 10.1021/acs.accounts.7b00510
Acc. Chem. Res. 2018, 51, 1054−1062

achieve an HER activity similar to that of commercial Pt/C.[44] This corresponds to a factor of 13 improvement in Pt mass activity and a 96% reduction in Pt loadings. We posited that CS NPs are more efficient than their thin film counterparts because of the higher surface density of Pt-TMC edge sites, allowing adjacent TMC surface sites to play an active role in both HER and HOR even at overpotentials below 10 mV.

Technoeconomic Analysis of NM/TMC NPs

Beyond access to novel catalytic reactivity, the ultimate goal of the CS NP architecture is to reduce costs associated with high NM catalyst loadings. HER in acidic media is one of the few reactions where highly active earth-abundant electrocatalysts, such as cobalt phosphide (CoP), have been designed to replace NMs altogether.[45] However, a cathode catalyst lifecycle analysis shows that 1/4 monolayer Pt/TiWC offers an overall factor of 6 reduction in costs compared to CoP and a factor of 12 reduction in costs compared to Pt/C (Figure 11). In fact, the cost of Pt in 1/4 monolayer Pt/TiWC is less than the cost of CoP required to achieve a similar HER activity. Thus, even for simple catalytic reactions where the use of NMs could be fully eliminated, we show the versatility of the CS NP architecture to deliver highly active, highly stable, and low-cost catalysts.

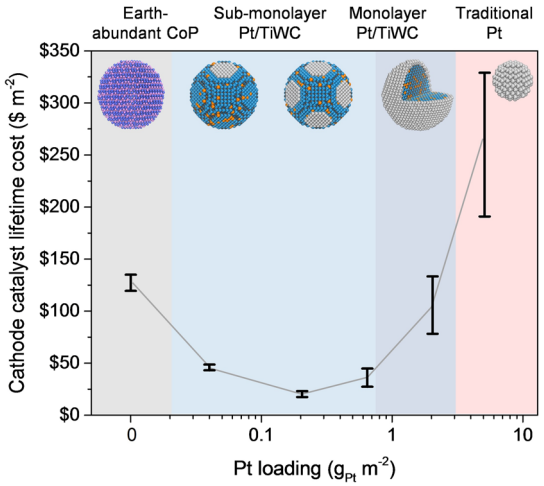

Figure 11. Technoeconomic analysis of HER electrocatalyst lifetime cost vs Pt loading. Sub-monolayer Pt/TiWC offers the lowest lifetime cost due to 96% lower Pt loadings without sacrificing HER activity. Error bars represent prediction intervals with 95% confidence. Adapted with permission from ref 44. Copyright 2016 Royal Society of Chemistry.

CONCLUSIONS AND OUTLOOK

Of the emerging NM catalyst architectures, core−shell NPs offer the most design flexibility to optimize catalyst activity, stability, and cost for both established and emerging technologies. Both transition metal carbides and nitrides exhibit a variety of ideal topochemical properties for supporting NM monolayers and satisfy most of the ideal core material constraints. However, they remain difficult to engineer. Although our computational and synthetic developments show that ceramics can serve in the capacity of ideal core candidates, new scalable manufacturing techniques are required for commercialization of not only NM/TMC NPs but the many other exciting emerging architectures.[18,46] Inexpensive and scalable synthesis of new architectures would improve the efficiency of current manufacturing processes, reducing greenhouse gas emissions. The cost of implementing new technologies such as fuel cells would no longer be dominated by catalyst loadings. We envision a future where computation and manufacturing advance to where ever better catalysts can be designed, manufactured, and released as simply as new software deployments.

AUTHOR INFORMATION

Corresponding Authors

*E-mail: seanhunt@alum.mit.edu.
*E-mail: yroman@mit.edu.

ORCID

Sean T. Hunt: 0000-0003-2966-2430
Yuriy Román-Leshkov: 0000-0002-0025-4233

Notes

The authors declare no competing financial interest.

Biographies

Sean Hunt received his B.S. and B.ChE. in Chemistry and Chemical Engineering from the University of Delaware in 2011 under the guidance of Prof. Jingguang Chen and his Ph.D. from MIT in 2016 under the guidance of Prof. Yuriy Román. Sean is a cofounder of Solugen, Inc., which seeks to commercialize green process technologies. Recently, he was featured in Forbes' 30 Under 30 and attended the Y Combinator winter 2017 batch.

Yuriy Román-Leshkov is an Associate Professor of Chemical Engineering at MIT. He received his Ph.D. from the University of Wisconsin-Madison in 2008 under the guidance of Prof. Jim Dumesic and completed his postdoctoral studies with Prof. Mark Davis at Caltech. At MIT, the Román Group specializes in elucidating the structure−activity relationships of heterogeneous catalysts and the design of novel catalytic materials.

REFERENCES

(1) *Handbook of heterogeneous catalysis*; 2nd ed.; Ertl, G., Knozinger, H., Schuth, F., Weitkamp, J., Eds.; John Wiley & Sons: Hoboken, NJ, 2008.
(2) Bell, A. T. The impact of nanoscience on heterogeneous catalysis. *Science* **2003**, *299*, 1688−1691.
(3) Adams, C. *About Catalysis*; North American Catalysis Society, January 19, 2012; http://nacatsoc.org/educational/about-catalysis/ (accessed January 2018).
(4) Gross Domestic Product 2016. In *World Development Indicators Database*; World Bank, December 15, 2017; http://databank.worldbank.org/data/download/GDP.pdf (accessed January 2018).
(5) Bravo-Suárez, J. J.; Chaudhari, R. V.; Subramaniam, B. In *Novel materials for catalysis and fuels processing*; American Chemical Society 2013, *1132*, 3−68.
(6) Zhang, J.; Everson, M. P.; Wallington, T. J.; Field, F. R., III; Roth, R.; Kirchain, R. E. Assessing economic modulation of future critical materials use: The case of automotive-related platinum group metals. *Environ. Sci. Technol.* **2016**, *50*, 7687−7695.
(7) Yang, C.-J. An impending platinum crisis and its implications for the future of the automobile. *Energy Policy* **2009**, *37*, 1805−1808.
(8) Wittstock, R.; Pehlken, A.; Wark, M. Challenges in automotive fuel cells recycling. *Recycling* **2016**, *1*, 343−364.
(9) Ghosh, P. C. High platinum cost: Obstacle or blessing for commercialization of low-temperature fuel cell technologies. *Clean Technol. Environ. Policy* **2017**, *19*, 595−601.
(10) Strasser, P.; Koh, S.; Anniyev, T.; Greeley, J.; More, K.; Yu, C.; Liu, Z.; Kaya, S.; Nordlund, D.; Ogasawara, H.; Toney, M. F.; Nilsson, A. Lattice-strain control of the activity in dealloyed core-shell fuel cell catalysts. *Nat. Chem.* **2010**, *2*, 454−460.

DOI: 10.1021/acs.accounts.7b00510
Acc. Chem. Res. 2018, 51, 1054−1062

(11) Somorjai, G. A.; Li, Y. *Introduction to surface chemistry and catalysis*, 2nd ed.; John Wiley & Sons: Hoboken, NJ, 2010.
(12) Holby, E. F.; Sheng, W.; Shao-Horn, Y.; Morgan, D. Pt nanoparticle stability in pem fuel cells: Influence of particle size distribution and crossover hydrogen. *Energy Environ. Sci.* **2009**, *2*, 865−871.
(13) Sasaki, K.; Naohara, H.; Choi, Y.; Cai, Y.; Chen, W. F.; Liu, P.; Adzic, R. R. Highly stable pt monolayer on pdau nanoparticle electrocatalysts for the oxygen reduction reaction. *Nat. Commun.* **2012**, *3*, 1115.
(14) Atanasoski, R. T.; Atankasoska, L. L.; Cullen, D. A. In *Electrocatalysis in fuel cells: A non- and low- platinum approach*; Shao, M., Ed.; Springer: London, 2013; p 637−664.
(15) Shrestha, S.; Mustain, W. E. In *Electrocatalysis in fuel cells: A non- and low- platinum approach*; Shao, M., Ed.; Springer: London, 2013, 689−728.
(16) Barnard, A. S.; Zapol, P. A model for the phase stability of arbitrary nanoparticles as a function of size and shape. *J. Chem. Phys.* **2004**, *121*, 4276−4283.
(17) Huang, R.; Shao, G.-F.; Zeng, X.-M.; Wen, Y.-H. Diverse melting modes and structural collapse of hollow bimetallic core-shell nanoparticles: A perspective from molecular dynamics simulations. *Sci. Rep.* **2015**, *4*, 7051.
(18) Chen, P.-C.; Liu, X.; Hedrick, J. L.; Xie, Z.; Wang, S.; Lin, Q.-Y.; Hersam, M. C.; Dravid, V. P.; Mirkin, C. A. Polyelemental nanoparticle libraries. *Science* **2016**, *352*, 1565−1569.
(19) Sasaki, K.; Mo, Y.; Wang, J. X.; Balasubramanian, M.; Uribe, F.; McBreen, J.; Adzic, R. R. Pt submonolayers on metal nanoparticles—novel electrocatalysts for H2 oxidation and O2 reduction. *Electrochim. Acta* **2003**, *48*, 3841−3849.
(20) Sasaki, K.; Naohara, H.; Cai, Y.; Choi, Y. M.; Liu, P.; Vukmirovic, M. B.; Wang, J. X.; Adzic, R. R. Core-protected platinum monolayer shell high-stability electrocatalysts for fuel-cell cathodes. *Angew. Chem., Int. Ed.* **2010**, *49*, 8602−8607.
(21) Hunt, S. T. *Engineering Carbide Nanoparticles Coated with Noble Metal Monolayers for Catalysis*; Massachusetts Institute of Technology, June 2016; http://hdl.handle.net/1721.1/104207 (accessed January 2017).
(22) Oyama, S. T. *The chemistry of transition metal carbides and nitrides*; Blackie: Glasgow, 1996.
(23) Kimmel, Y. C.; Xu, X.; Yu, W.; Yang, X.; Chen, J. G. Trends in electrochemical stability of transition metal carbides and their potential use as supports for low-cost electrocatalysts. *ACS Catal.* **2014**, *4*, 1558−1562.
(24) Levy, R. B.; Boudart, M. Platinum-like behavior of tungsten carbide in surface catalysis. *Science* **1973**, *181*, 547−549.
(25) Ribeiro, F. H.; Boudart, M.; Betta, R. A. D. Catalytic reactions of n-alkanes on β-W2C and WC: The effect of surface oxygen on reaction pathways. *J. Catal.* **1991**, *130*, 498−513.
(26) Stottlemyer, A. L.; Kelly, T. G.; Meng, Q.; Chen, J. G. Reactions of oxygen-containing molecules on transition metal carbides: Surface science insight into potential applications in catalysis and electrocatalysis. *Surf. Sci. Rep.* **2012**, *67*, 201−232.
(27) Michalsky, R.; Zhang, Y. J.; Medford, A. J.; Peterson, A. A. Departures from the adsorption energy scaling relations for metal carbide catalysts. *J. Phys. Chem. C* **2014**, *118*, 13026−13034.
(28) Yan, Z.; Cai, M.; Shen, P. K. Nanosized tungsten carbide synthesized by a novel route at low temperature for high performance electrocatalysis. *Sci. Rep.* **2013**, *3*, 1646.
(29) Hsu, I. J.; Kimmel, Y. C.; Jiang, X.; Willis, B. G.; Chen, J. G. Atomic layer deposition synthesis of platinum-tungsten carbide core-shell catalysts for the hydrogen evolution reaction. *Chem. Commun.* **2012**, *48*, 1063−1065.
(30) Ganesan, R.; Lee, J. S. Tungsten carbide microspheres as a noble-metal-economic electrocatalyst for methanol oxidation. *Angew. Chem., Int. Ed.* **2005**, *44*, 6557−6560.
(31) Ivanovskii, A. L. Platinum group metal nitrides and carbides: Synthesis, properties and simulation. *Russ. Chem. Rev.* **2009**, *78*, 303−318.
(32) Esposito, D. V.; Hunt, S. T.; Stottlemyer, A. L.; Dobson, K. D.; McCandless, B. E.; Birkmire, R. W.; Chen, J. G. Low-cost hydrogen-evolution catalysts based on monolayer platinum on tungsten monocarbide substrates. *Angew. Chem., Int. Ed.* **2010**, *49*, 9859−9862.
(33) Esposito, D. V.; Hunt, S. T.; Kimmel, Y. C.; Chen, J. G. A new class of electrocatalysts for hydrogen production from water electrolysis: Metal monolayers supported on low-cost transition metal carbides. *J. Am. Chem. Soc.* **2012**, *134*, 3025−3033.
(34) Kelly, T. G.; Hunt, S. T.; Esposito, D. V.; Chen, J. G. Monolayer palladium supported on molybdenum and tungsten carbide substrates as low-cost hydrogen evolution reaction (her) electrocatalysts. *Int. J. Hydrogen Energy* **2013**, *38*, 5638−5644.
(35) Hunt, S. T.; Milina, M.; Alba-Rubio, A. C.; Hendon, C. H.; Dumesic, J. A.; Roman-Leshkov, Y. Self-assembly of noble metal monolayers on transition metal carbide nanoparticle catalysts. *Science* **2016**, *352*, 974−978.
(36) Hendon, C. H.; Hunt, S. T.; Milina, M.; Butler, K. T.; Walsh, A.; Roman-Leshkov, Y. Realistic surface descriptions of heterometallic interfaces: The case of tiwc coated in noble metals. *J. Phys. Chem. Lett.* **2016**, *7*, 4475−4482.
(37) Vayenas, C.; Bebelis, S.; Ladas, S. Dependence of catalytic rates on catalyst work function. *Nature* **1990**, *343*, 625−627.
(38) Hammer, B.; Morikawa, Y.; Norskov, J. Co chemisorption at metal surfaces and overlayers. *Phys. Rev. Lett.* **1996**, *76*, 2141−2144.
(39) Hunt, S. T.; Nimmanwudipong, T.; Roman-Leshkov, Y. Engineering non-sintered, metal-terminated tungsten carbide nanoparticles for catalysis. *Angew. Chem., Int. Ed.* **2014**, *53*, 5131−5136.
(40) Hunt, S. T.; Roman-Leshkov, Y. Reverse microemulsion-mediated synthesis of monometallic and bimetallic early transition metal carbide and nitride nanoparticles. *J. Visualized Exp.* **2015**, e53147.
(41) Joo, S. H.; Park, J. Y.; Tsung, C.-K.; Yamada, Y.; Yang, P.; Somorjai, G. a. Thermally stable pt/mesoporous silica core-shell nanocatalysts for high-temperature reactions. *Nat. Mater.* **2009**, *8*, 126−131.
(42) Hunt, S. T.; Kokumai, T. M.; Zanchet, D.; Roman-Leshkov, Y. Alloying tungsten carbide nanoparticles with tantalum: Impact on electrochemical oxidation resistance and hydrogen evolution activity. *J. Phys. Chem. C* **2015**, *119*, 13691−13699.
(43) Garg, A.; Milina, M.; Ball, M.; Zanchet, D.; Hunt, S. T.; Dumesic, J. A.; Román-Leshkov, Y. Transition-metal nitride core@noble-metal shell nanoparticles as highly co tolerant catalysts. *Angew. Chem., Int. Ed.* **2017**, *56*, 8828−8833.
(44) Hunt, S. T.; Milina, M.; Wang, Z.; Roman-Leshkov, Y. Activating earth-abundant electrocatalysts for efficient, low-cost hydrogen evolution/oxidation: Sub-monolayer platinum coatings on titanium tungsten carbide nanoparticles. *Energy Environ. Sci.* **2016**, *9*, 3290−3301.
(45) Popczun, E. J.; Read, C. G.; Roske, C. W.; Lewis, N. S.; Schaak, R. E. Highly active electrocatalysis of the hydrogen evolution reaction by cobalt phosphide nanoparticles. *Angew. Chem., Int. Ed.* **2014**, *53*, 5427−5430.
(46) Tackett, B. M.; Sheng, W.; Chen, J. G. Opportunities and challenges in utilizing metal-modified transition metal carbides as low-cost electrocatalysts. *Joule* **2017**, *1*, 253−263.

DOI: 10.1021/acs.accounts.7b00510
Acc. Chem. Res. 2018, 51, 1054−1062